

Localization of Structure on Extended RO Propagation Geometries

Charles L. Rino, Charles S. Carrano, and Keith M. Groves
Boston College, Institute for Scientific Research, Chestnut Hill, MA

Version: May 1, 2017

GPS-to-low-earth-orbiting (LEO) radio occultation (RO) geometries are designed for vertical-plane measurements. Reconstruction of atmospheric and ionospheric profiles is facilitated by the planar geometry. Interpreting scintillation that develops over the extended propagation path is more challenging. The point of closest approach is a natural reference for reporting scintillation on occultation paths. However, the structure variation provides information that can be exploited to localize the structure along the extended path. Carrano, et al. demonstrated the principle. A companion presentation will discuss more recent results based on Irregularity Parameter Estimation (IPE).

A configuration-space model has been developed that generates ionospheric structure realizations from distributions of magnetic-field-aligned striations. The striation size distribution can be structured to generate one or two-component inverse power law spectral distributions. The model can populate a representative volume that captures the occultation plane. The model is being applied to investigate the structure configurations that can be resolved by interpreting the occultation intensity variation. Our preliminary results confirm that the ideal field-crossing geometry works well. In this paper we will investigate localization for a range of representative RO geometries.

Key Words: GPS, Scintillation, Modeling, Numerical Simulation

1. INTRODUCTION

Propagation in extended media has been investigated with multiple-phase-screen simulations [1]. However, the phase-screens are typically populated with statistically independent isotropic structure. While this is appropriate for two-dimensional propagation normal to the field lines, a complete propagation model must accommodate three-dimensional propagation in an extended highly anisotropic medium. To illustrate the environment, Figure 1 shows a snapshot of a high-resolution equatorial plasma bubble simulation [2]. The evolving structure maps along field lines connecting the vertical equatorial plane to oblique slice planes ending at the bottom of the F layer in opposite hemispheres. Stochastic structure can be characterized only in two-dimensional slice planes that capture enough structure variation to support average coherence measures.

A configuration-space model was developed to generate ionospheric structure realizations with collections of randomly located striations. Striations characterize the ionization along specified field lines. By selecting appropriate striation scale and fractional intensity distributions, configuration-space realizations support two-dimensional multi-component inverse-power-law spectral density functions (SDFs). A detailed description can be found in the paper <http://chuckrino.com/wordpress/wp-content/uploads/2015/04/ConfigurationSpaceModelsREV11.pdf>, which has been submitted for publication. This paper will describe propagation simulations designed

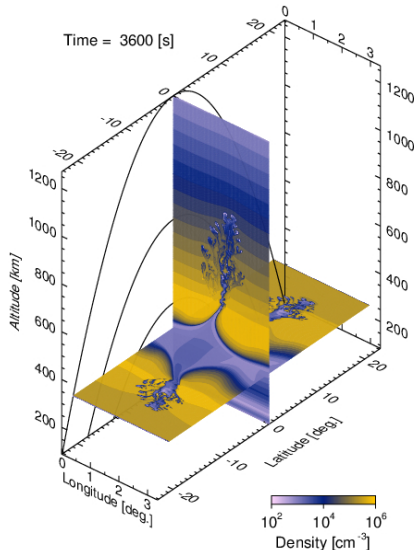


FIG. 1 Field-aligned geometry for high-resolution simulation of equatorial plasma bubbles.

to investigate the phase-screen approximation and two-dimensional propagation models that exploit field-aligned anisotropy as well as phase-screen equivalence.

The configuration-space model populates a rectangular data space volume with a reference axis along the direction of propagation. Let $\Delta N(x; y, z)$ represent the ionization in an yz plane at distance x from an arbitrary reference in the structured region. Propagation simulations are constructed by using split-step parabolic-wave-equation (PWE) integration within the structure region, followed by free-space propagation to an observation plane. There is no loss of generality in choosing the reference axis as the propagation direction as long as measurements are confined to planes normal to the propagation direction. Oblique propagation can be used as well [3]. The choice is characterizing the structure in an arbitrarily oriented coordinate system versus using a fixed coordinate system in which both the propagation direction and the direction of the magnetic field are arbitrary.

2. PROPAGATION SIMULATIONS

For this study simulations were run with varying magnetic field direction relative to the reference axis. The realizations were defined by $64 \times 4096 \times 4096$ samples spanning 30 km along x , 50 km along y , and 50 km along z . The coarser x sampling is matched to split-step integration, which requires only that the intensity change be small. Each realization is comprised of 8188 striations with scales from 20 km to 20 m. The striations were configured to support the canonical one-dimensional inverse power law $C_s q^{-2}$. The single-power-law was chosen for ease of interpretation. Figure 2 shows the measured average one-dimensional cross-field SDF (red) with the theoretical curve overlaid (blue). The inverse-power-law range spans the spatial-frequency range from more than 10 km to less than 100 m.

Simulations were run at the GPS L1 frequency 1575.4 MHz. To track the

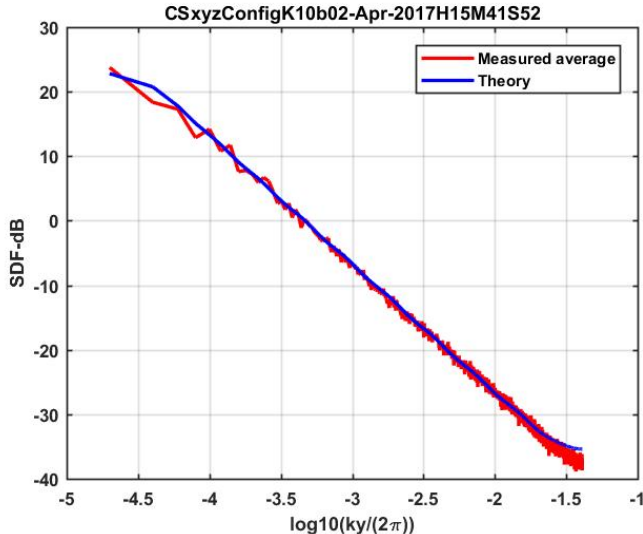


FIG. 2 Comparison of measured 1 D average cross-fied SDF (red) with theory (blue).

scintillation development S4 estimates were generated at each integration step and at logarithmically spaced free-space intervals to a measurement plane at 138 km. Figure 3 summarizes the structure evolution at for full-diffraction (red structure, blue free space) and phase-screen (magenta structure, green free space) calculations. The three frames show varying propagation angles relative to the magnetic field (cross field upper frame, 60 degrees middle frame, and field-aligned, lower frame). The phase-screen results are offset by half the width of the structured region. The offset aligns the phase-screen results with the full-diffraction results once the full diffraction level is achieved at one-half the layer thickness.

The intensity structure in the measurement planes are show in Figure 4. The cross-field geometry is invariant along the magnetic field direction. As the propagation angle decreases from 90 degrees the measurement plan structure evolves from one-dimensional to isotropic. Because only the orientation of the magnetic field direction was varied, coherence along the propagation direction increases, which leads to extreme departures from uniform structure. The circular diffraction detail is not visible in the lower frame of Figure 4, but it accounts for the unrealistically low S4 values in the lower frame of Figure 3. The striation profile structure becomes more important as field-aligned propagation is approached.

To interpret the crossing results we employ the phase-screen theory as described in Carrano and Rino [4]. The theory predicts the intensity SDF in $I(\mu)$, where $\mu = q\rho_F$, and q is the spatial wavenumber in radians per meter. The normalized parameters that define the equivalent phase SDF are $C_{pp} = C_p \rho_F^{p_1 - 1}$, p_1 , $\mu_0 = q_0 \rho_F$, and p_2 . That is,

$$P(\mu) = C_{pp} \begin{cases} \mu^{-p_1} & \text{for } \mu_0 \geq 1 \\ \mu_0^{p_2 - p_1} \mu^{-p_2} & \text{for } \mu_0 < 1 \end{cases} \quad (1)$$

The C_{pp} parameter is absorbed in a monotonic universal strength parameter U ,

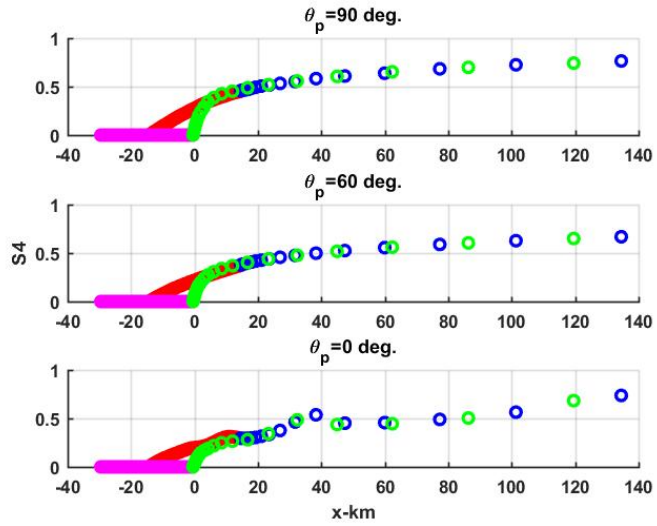


FIG. 3 S_4 evolution for full-diffraction (red-blue) and phase-screen calculations (magenta-green).

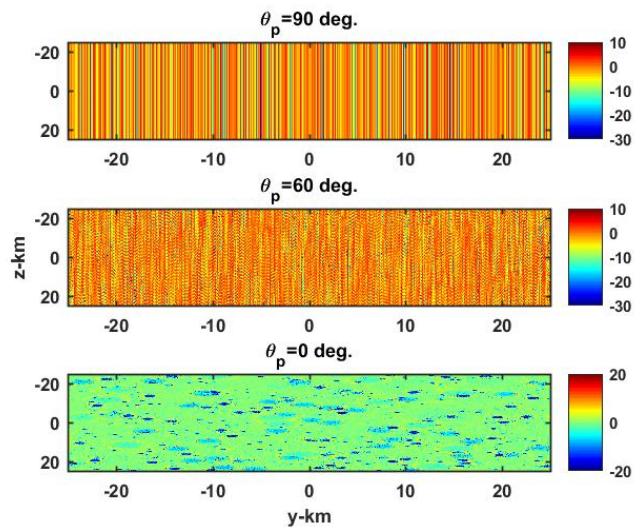


FIG. 4 Field intensity in measurement plane at 138 km.

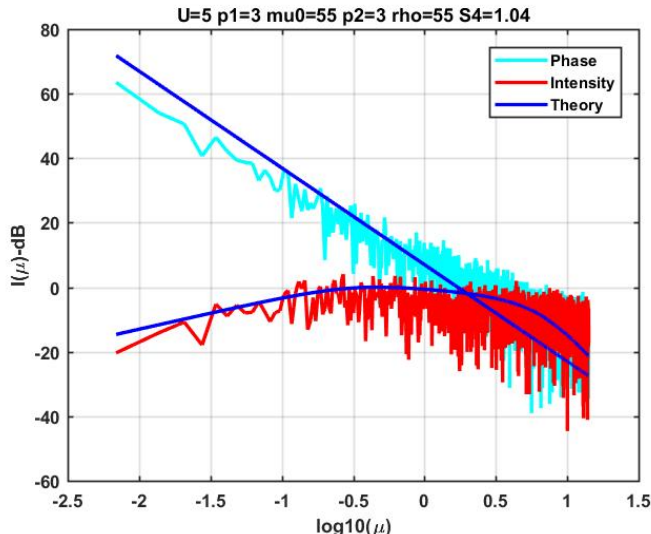


FIG. 5 Measured intensity (red) and phase (cyan) SDFs with phase-screen theory integrated phase and intensity SDFs overlaid (blue).

which orders perturbation strength: $U < 1$ corresponds to weak to moderate scintillation. $U > 1$ corresponds to strong scintillation. To relate the phase-screen parameters to the defining in-situ structure parameters, we $p_1 = p_2 = 3$. The relation depends on decorrelation along the path-integration direction. The free parameters are U and ρ_F . Effectively, ρ_F centers the theoretical SDF while U adjusts the strength to match the theoretical and measured S_4 index. The following table summarizes the results for the cross-field and 60 degree simulations.

Simulation	U	ρ_F	S_4 Theory	S_4 Meas
$\theta_p = 90$ Full	1.2	60	0.73	0.77
$\theta_p = 90$ Screen	0.8	55	0.61	0.65
$\theta_p = 60$ Full	1	60	0.67	0.68
$\theta_p = 60$ Screen	0.8	55	0.61	0.59

The fact that the phase-screen results are somewhat smaller than the full-diffraction computation is attributed to the shorted effective propagation distance. There is some sensitivity to the aspect direction as well. However, it may be that the increased coherence along the propagation direction is changing the relation between the one-dimensional in-situ index and the phase-screen index. At this point the general overall agreement is encouraging. As a final check the cross-field perturbation strength was increased by an order of magnitude. Scaling the structure realization should only change U . Figure 5 shows the intensity SDF with the theoretical SDF for the parameters summarized in the figure label. The measured S_4 value was 1.05. The simulation captures the expected broadening of the intensity SDF. For completeness the theoretical phase-screen SDF is plotted together with the SDF of the phase scintillation. There is no theory that predicts the phase SDF, particularly under strong-scatter conditions, but correspondence between the phase SDF (cyan) and the phase-screen SDF (blue) is noteworthy.

3. DISCUSSION

The configuration-space results presented in this paper show that at least for the canonical single-component inverse-power-law SDF the full-diffraction and phase-screen results are statistically equivalent as long as the propagation angle is not too close to field-aligned. The behavior approaching field alignment needs further study. We also showed that both the full-diffraction and the phase-screen results could be reconciled with the two-dimensional phase screen theory. In particular, we verified the expected structure changes with increasing perturbation strength.

The question of whether the results could have been deduced without prior knowledge of the structure parameters remains a topic of further study. Similarly, the ramifications of correlated structure along the propagation direction and the mapping of two-component in-situ spectra onto equivalent phase structure remains to be investigated. There is evidence that the ideal mapping that simply increases the one-dimensional in-situ index by one might be distorted.

REFERENCES

- [1] Dennis L. Knepp. Multiple phase-screen calculation of the temporal behavior of stochastic waves. *Radio Sci.*, 71(6), 1983.
- [2] Tatsuhiro Yokoyama and Claudia Stolle. Low and midlatitude ionospheric plasma density irregularities and their effects on geomagnetic field. *Space Sci Rev*, (doi:10.1007/s11214-016-295-7), 2016.
- [3] K. B. Deshpande, G. S. Bust, C. R. Clauer, C. L. Rino, and C. S. Carrano. Satellite-beacon ionospheric-scintillation global model of the upper atmosphere (σ_{z}): High-latitude sensitivity study of the model parameters. *J. Geophys. Res. Space Physics*, 119(doi:10.1002/2013JA019699):4026–4043, 2014.
- [4] C. S. Carrano and C. L. Rino. A theory of scintillation for two-component power law irregularity spectra: Overview and numerical results. *Radio Sci.*, 51(doi:10.1002/2015RS005903):789–813, 2016.